Measurements of 50 Double Stars with 25 and 30-cm Refractors

Roger C. Ceragioli
University of Arizona, Tucson, AZ; lensbender@msn.com

Abstract

The present article forms a continuation of the author's first report, published in the April 2023 issue of the *Journal of Double Star Observations*.[1] Since those observations were concluded, the author has continued taking measurements, initially using the same 254-mm apochromatic refractor described there, but later employing a newly completed 310-mm achromatic refractor, folded into a compact 1.5-meter long configuration. This new instrument has proven excellent, as the images included in the present report will show. Since May 2023, the author has used this larger refractor exclusively, both for visual observation and for double-star measurements. It gradually became clear that by careful technique, this telescope could successfully image close doubles in the southern sky, down to a declination of about -30°. This has opened the possibility of examining some neglected van den Bos and Rossiter pairs. The present report discusses the techniques employed to achieve this, and lists measures of 50 doubles and triples made by the author from January through early July 2023. Appended is an "atlas" or table of images for all the stars measured.

1. Introduction

The author designed and built a 310-mm f/15 achromatic refractor in 2022-23. Ordinarily, such a classic type of instrument would have required an enormous tube and mounting, as was customary in the 19th c. Instead, the author "folded" the light path using flat mirrors, allowing a much abbreviated tube. Figure 1 shows the ray-path of the system, with the achromatic doublet objective depicted at lower left, and three folding flats in succession. The focus falls at upper right where the rays (blue lines) converge to a point. The author built the lenses, mirrors, and complete tube assembly.

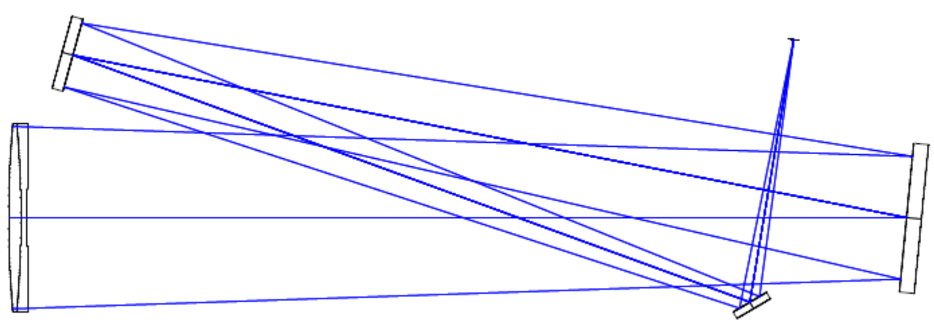

Figure 1: Ray-path of 310-mm f/15 folded refractor

1. Ceragioli, R.C., "Measurements of 26 Double Stars with a 254-mm Refractor," *JDSO*, 19.2 (2023), pp. 150-158.

The completed tube assembly is shown in Figure 2. It easily fits on an Astro-Physics™ 1100GTO telescope mounting, and can be set up and taken down nightly, as needed.

Figure 2: Completed tube assembly of 310-mm f/15 folded refractor on AP-1100 mounting

To image stars with this telescope, a ZWO ASI290 monochrome CMOS camera (depicted in Figure 2) has been used exclusively, together with a yellow filter (Wratten #12). The latter removes unfocused light (secondary spectrum), as found in all achromatic refractors, and eliminates the need for an atmospheric dispersion corrector (ADC) when observing at a low altitude. In the course of using the earlier 254-mm apochromatic refractor, the author discovered how sensitive it was to such dispersion, which visibly elongated star images. This can be detected in the first five stellar systems (STF296AB to HO511AC) illustrated in the “atlas” of images, placed at the end of the present report (see Section 6 below), all of which were taken with the 254-mm apochromatic refractor. The rest of the systems were imaged with the 310-mm achromat. With both of these telescopes, a hexagonal mask was placed over the aperture to reshape the diffraction pattern and divert light from its rings, making faint companions near brighter primaries more easily visible.[2]

2 *Cf.* Argyle, R., (2012), “The Resolution of a Telescope,” in *Observing and Measuring Visual Double Stars*, p. 110.

2. Calibration and Method of Data Collection for this Report

A critical parameter in CCD metrology is the image scale (in arcseconds/pixel). This was evaluated as discussed in the author's first report, by applying a diffraction mask to the 310-mm objective, consisting of a grating with alternating dark-and-light bars. The same grating was employed on the 254-mm refractor, and was illustrated in the author's earlier report. With the 310-mm objective, the constant *E* was found to be 0.1292 arcsec/pixel when using the ZWO ASI290 camera (with 2.9-micron pixels), which implies an effective focal length of 4630 mm for the 310-mm achromat, giving an adequate image scale without the need for a Barlow lens.

The general method of proceeding in the present research was identical to what the author described in his first report, except that here, all image grading, stacking, and other processing was carried out with F. Losse's program *REDUC*. "FITS Cubes" of *ca*. 2000 frames each were taken via *FireCapture*, and opened directly into *REDUC*. After finding a subframe that showed both stars to be measured (sometimes after utilizing the "BestOf (Vis)" function) clearly enough, search boxes of suitable size were placed around them and the "ELI" or "Easy Lucky Imaging" tool was invoked. This automatically grades the frames, rejects some, and ultimately stacks those accepted with a view to reinforcing the stars and sharpening them. In the end, ELI allows different percentages of accepted frames to be stacked, which smooths but may also dilute the image cores. The user selects the stacking percentage that seems best for the given FITS Cube, and saves the result as a small FITS file.

Once all the Cubes have been processed, the user opens the reduced FITS files and measures them in the usual way, either by manually pointing and clicking on the sharpened star images or allowing *REDUC* to measure them automatically via the "AutoReduc" function (as explained in the online user's manual). The user can also perform speckle interferometry on the FITS Cubes and save separate files for measurement. Both methods were employed in the present research, in varying amounts, on a case-by-case basis. The "means" thus produced are what one finds in Tables 2 and 3 below.

Over the course of months and after trying other methods of image processing, the author found empirically that *REDUC*'s "ELI" function, performed on FITS Cubes appeared to give the best (that is, sharpest and cleanest) star images, allowing the clearest separation of close doubles with his equipment.

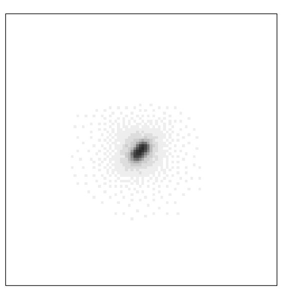

Figure 3: STT208 (Phi UMa)

An example is given in Figure 3 above, showing the close, nearly equal pair STT208 (Phi UMa). This pair of 5th magnitude stars is currently separated by 0.45 arcsec, and lies near the Dawes' limit (0.37 arcsec) of the 310 mm aperture. STT208 is rather clearly split in the above figure, and was even more so by visual inspection on the night of May 24, 2023, when the above image was made. That image is the result of collecting and processing ten FITS Cubes of ca. 2000 frames each, reducing them with ELI, and then further stacking the resultant smaller FITS files. When measured in *REDUC* (and by working from the individual FITS files), the separation of the components was found to be on average 0.44 arcsec, closely matching the Washington Double Star Catalog's (WDS) ephemeris for the star (*cf.* Tables 2 and 4 below).

3. Data Acquired

The following tables summarize the data, and their probable errors. In Table 1, we have numbers derived from the WDS for comparison. From left to right, we find in the first column the WDS 9-digit identifier. In column two appears the discoverer's code and catalog number. The third and fourth columns present the WDS-listed magnitudes of the primary and secondary stars. The fifth column gives the magnitude difference. The sixth and seventh columns list the position angles (θ) in degrees, and separations (ρ) in arcseconds of the stars, according to the latest observation contained in the WDS, measured in the year specified in the eighth and final column.

Table 1. WDS data on the doubles measured for the present report

WDS ID	Name	M1	M2	ΔM	WDS θ	WDS ρ	Year
02442+4914	STF296AB	4.16	10	5.84	306.1	21.15	2020
05003+3924	STT92AB	6.02	9.50	3.48	285.0	4.08	2017
05013+5015	STF619	9.51	9.88	0.37	161.7	4.23	2021
05172+3246	COU1088	10.16	11.54	1.38	233.0	1.67	1991
06012+3516	HU826AB	10.13	10.26	0.13	303.6	0.48	1992
06012+3516	HO511AC	10.13	11.8	1.67	173.4	4.01	2016
09521+5404	STT208	5.28	5.39	0.11	316.9	0.48	2022
12115+5325	STF1608AB	8.11	8.27	0.16	220.5	13.60	2021
12272+2701	STF1643AB	9.03	9.45	0.42	3.10	2.76	2020
12412-0127	BU607	9.7	11.9	2.2	307.7	0.89	1982
12533+2115	STF1687AB	5.15	7.08	1.93	202.8	1.20	2020
12533+2115	STF1687AC	5.15	9.76	4.61	127.1	28.50	2016
13026+2318	COU95	9.7	11.3	1.6	286.1	0.70	2013
13076-1415	RST3820	10.5	11.2	0.7	253.1	0.81	1943
13120+3205	STT261	7.4	7.64	0.24	337.4	2.53	2020
13152-1004	A2781	10.4	12.3	1.9	358.5	0.91	1989
13166+5034	STT263	9.53	9.74	0.21	137.5	1.75	2019
13169+1701	BU800AB	6.66	9.50	2.84	104.1	7.65	2020
13181-1820	RST2839AB	9.7	11.3	1.6	47.5	0.50	1960
13199-2748	B247	9.56	12.7	3.14	316.6	2.54	1960
13284+1543	STT266	7.97	8.42	0.45	355.3	1.92	2020
13298-2634	B250	8.5	9.5	1.0	46.9	0.53	1990
13375+3618	STF1768AB	4.98	6.95	1.97	94.5	1.62	2020

13400-1914	RST2858	10.4	11.2	0.8	235.9	0.66	1940
13403-1913	RST2859	10.45	10.70	0.25	123.3	2.34	2016
13491+2659	STF1785	7.36	8.15	0.79	192.6	2.72	2021
14095-2205	RST2891	10.4	12.7	2.3	141.0	0.93	2016
14165+2007	STF1825	6.47	8.42	1.95	153.9	4.22	2019
14247-1140	STF1837	6.87	7.94	1.07	270.0	1.27	2016
14271-1505	RST3879	10.4	12.6	2.2	110.1	0.71	1943
14314+8257	MLR337	9.90	11.62	1.72	167.2	2.17	2022
14381-0841	BU804	8.69	11.10	2.41	134.6	1.29	2016
14447-0712	RST3893	10.28	11.44	1.16	179.0	0.64	1991
14493-1409	BU106AB	5.61	6.62	1.01	7.3	1.94	2019
14579-2834	B283	10.3	10.7	0.4	247.4	0.47	1962
15023-0858	RST3903	10.31	12.3	1.99	122.5	1.25	2016
15055+5707	A1113	9.6	12.3	2.7	317.3	0.72	2016
15055-0701	BU119AB	8.09	8.76	0.67	273.9	2.33	2019
15199+6701	HU1161AB	8.05	10.87	2.82	224.8	1.67	1991
15304-2717	B292AB	9.11	12.3	3.19	103.6	1.82	1965
15304-2717	B292AC	9.11	12.83	3.72	97.7	15.33	2016
15484-2210	B2370	10.3	11.7	1.4	92.8	0.50	1959
16006-2027	HLD126	9.66	11.72	2.06	34.2	2.29	1991
16009+1918	A2081AB	9.08	12.4	3.32	321.0	2.42	1987
16011+6531	HU1170	9.73	11.27	1.54	147.1	1.13	1991
16044-1122	STF1998AB	4.84	4.86	0.02	11.9	1.15	2020
16044-1122	STF1998AC	4.84	7.30	2.46	44.6	7.15	2019
16044-1122	STF1998BC	4.86	7.30	2.44	37.5	8.77	2019
16096-2037	HU660	8.6	11.8	3.2	67.3	2.57	1965
16359-2510	RST3033	9.3	11.5	2.2	145.7	0.58	1940

Table 2 presents the author's measured data. Column one and two reprise the WDS ID and discoverer codes. Columns three and four present the author's measured position angles and separations. These are averages of all the ELI and speckle images. Column five lists the Julian epoch (JE) of observation. And columns six and seven give the number of ELI and speckle images, and the number of nights on which the star was observed. When more than one night is indicated, the θ, ρ, and JE are averages of the individual nights.

Table 2. Author's measurements.

WDS ID	Name	Obs. θ	Obs. ρ	JE	#Ims	#Nts
02442+4914	STF296AB	305.3°	21.19″	2023.02	11	1
05003+3924	STT92AB	284.9°	4.20″	2023.17	9	1
05013+5015	STF619	162.6°	4.24″	2023.17	10	1
05172+3246	COU1088	223.5°	1.47″	2023.10	30	3
06012+3516	HU826AB	312.4°	0.80″	2023.14	13	2

06012+3516	HO511AC	173.6°	4.03″	2023.14	13	2
09521+5404	STT208	315.8°	0.44″	2023.39	10	1
12115+5325	STF1608AB	220.5°	13.57″	2023.38	5	1
12272+2701	STF1643AB	2.0°	2.80″	2023.40	14	2
12412-0127	BU607	300.7°	0.86″	2038.40	12	1
12533+2115	STF1687AB	204.6°	1.16″	2023.42	32	3
12533+2115	STF1687AC	126.7°	28.63″	2023.44	10	1
13026+2318	COU95	278.9°	0.70″	2023.39	15	2
13076-1415	RST3820	249.9°	0.81″	2023.45	6	1
13120+3205	STT261	338.8°	2.66″	2023.39	11	1
13152-1004	A2781	7.3°	0.72″	2023.44	6	1
13166+5034	STT263	136.6°	1.72″	2023.42	11	1
13169+1701	BU800AB	104.4°	7.73″	2023.39	10	1
13181-1820	RST2839AB	30.4°	0.60″	2023.42	6	1
13199-2748	B247	308.8°	4.26″	2023.45	5	1
13284+1543	STT266	358.8°	1.97″	2023.42	11	1
13298-2634	B250	43.3°	0.52″	2023.46	14	2
13375+3618	STF1768AB	93.9°	1.67″	2023.40	12	1
13400-1914	RST2858	224.8°	0.55″	2023.42	6	1
13403-1913	RST2859	123.2°	2.35″	2023.42	5	1
13491+2659	STF1785	194.1°	2.62″	2023.41	12	1
14095-2205	RST2891	142.4°	0.82″	2023.45	5	1
14165+2007	STF1825	151.8°	4.35″	2023.41	12	1
14247-1140	STF1837	268.1°	1.10″	2023.49	12	1
14271-1505	RST3879	111.3°	0.77″	2023.45	5	1
14314+8257	MLR337	167.1°	2.14″	2023.40	5	1
14381-0841	BU804	134.0°	1.23″	2023.40	7	1
14447-0712	RST3893	174.8°	0.54″	2023.41	5	1
14493-1409	BU106AB	8.4°	1.89″	2023.48	21	2
14579-2834	B283	234.9°	0.52″	2023.48	20	2
15023-0858	RST3903	125.2°	1.12″	2023.46	11	2
15055+5707	A1113	317.6°	0.66″	2023.48	8	1
15055-0701	BU119AB	273.8°	2.34″	2023.51	12	1
15199+6701	HU1161AB	227.0°	1.40″	2023.51	11	1
15304-2717	B292AB	106.2°	1.87″	2023.45	5	1
15304-2717	B292AC	97.1°	15.55″	2023.45	5	1
15484-2210	B2370	89.6°	0.55″	2023.47	8	1
16006-2027	HLD126	39.5°	2.07″	2023.51	4	1
16009+1918	A2081AB	324.5°	2.44″	2023.48	10	1
16011+6531	HU1170	147.8°	0.86″	2023.51	6	1
16044-1122	STF1998AB	16.5°	1.03″	2023.51	10	1
16044-1122	STF1998AC	41.5°	8.02″	2023.51	11	1
16044-1122	STF1998BC	45.0°	7.11″	2023.51	10	1

16096-2037	HU660	59.4°	3.94″	2023.47	12	1
16359-2510	RST3033	139.6°	0.73″	2023.51	9	1

Table 3 indicates the statistical errors, specifying the standard deviations (SD) of position angle (θ) and separation (ρ), together with the standard errors of the mean (SEM), derived from the author's measures. The standard deviations come directly from *REDUC*. The standard errors were computed by the author. Where the double star in question was observed on more than one night, these are averages of the individual nights. As usual in such measurements, the largest SDs occur with the position angles of close doubles, as for example B250, whose separation is about 0.5 arcsec.

Table 3. Measurement errors.

WDS ID	Name	θ SD	θ SEM	ρ SD	ρ SEM
02442+4914	STF296AB	0.31	0.093	0.11	0.033
05003+3924	STT92AB	0.17	0.057	0.02	0.005
05013+5015	STF619	0.15	0.046	0.01	0.003
05172+3246	COU1088	0.74	0.135	0.03	0.005
06012+3516	HU826AB	1.95	0.541	0.05	0.013
06012+3516	HO511AC	0.31	0.086	0.02	0.006
09521+5404	STT208	1.48	0.466	0.04	0.011
12115+5325	STF1608AB	0.09	0.040	0.05	0.021
12272+2701	STF1643AB	0.22	0.059	0.02	0.005
12412-0127	BU607	0.66	0.189	0.01	0.004
12533+2115	STF1687AB	0.87	0.154	0.04	0.007
12533+2115	STF1687AC	0.08	0.025	0.04	0.014
13026+2318	COU95	1.39	0.065	0.03	0.008
13076-1415	RST3820	1.41	0.574	0.03	0.013
13120+3205	STT261	0.21	0.063	0.02	0.005
13152-1004	A2781	2.92	1.192	0.05	0.019
13166+5034	STT263	0.59	0.176	0.02	0.005
13169+1701	BU800AB	0.14	0.044	0.03	0.009
13181-1820	RST2839AB	3.30	1.347	0.05	0.021
13199-2748	B247	1.04	0.465	0.13	0.057
13284+1543	STT266	0.15	0.045	0.01	0.003
13298-2634	B250	4.15	1.109	0.05	0.013
13375+3618	STF1768AB	0.43	0.123	0.01	0.003
13400-1914	RST2858	1.26	0.512	0.03	0.014
13403-1913	RST2859	0.68	0.302	0.04	0.018
13491+2659	STF1785	0.32	0.091	0.02	0.005
14095-2205	RST2891	1.70	0.758	0.03	0.015
14165+2007	STF1825	0.25	0.072	0.02	0.007
14247-1140	STF1837	1.21	0.349	0.03	0.009
14271-1505	RST3879	1.74	0.778	0.01	0.006

14314+8257	MLR337	0.66	0.295	0.05	0.022
14381-0841	BU804	2.19	0.828	0.05	0.017
14447-0712	RST3893	0.76	0.340	0.01	0.006
14493-1409	BU106AB	0.33	0.071	0.03	0.005
14579-2834	B283	3.38	0.755	0.04	0.009
15023-0858	RST3903	1.62	0.487	0.05	0.015
15055+5707	A1113	4.08	1.441	0.06	0.020
15055-0701	BU119AB	0.48	0.137	0.02	0.005
15199+6701	HU1161AB	1.75	0.528	0.07	0.021
15304-2717	B292AB	1.00	0.449	0.08	0.036
15304-2717	B292AC	0.26	0.116	0.09	0.040
15484-2210	B2370	1.79	0.631	0.02	0.007
16006-2027	HLD126	0.42	0.210	0.03	0.016
16009+1918	A2081AB	0.74	0.232	0.05	0.015
16011+6531	HU1170	1.10	0.447	0.03	0.012
16044-1122	STF1998AB	0.34	0.108	0.02	0.006
16044-1122	STF1998AC	0.15	0.045	0.03	0.009
16044-1122	STF1998BC	0.16	0.051	0.04	0.012
16096-2037	HU660	0.58	0.166	0.05	0.014
16359-2510	RST3033	2.42	0.807	0.09	0.030

4. Discussion and Notes

Table 4 shows the residuals of the author's measurements from the last WDS published data, as well as from the orbital ephemeris (if one exists). The first and second columns are as in the previous tables. The third and fourth give the residuals, showing the author's observations minus the most recent WDS data, and the author's work minus the current (2023) ephemeris position, respectively. The ephemerides come from Matson, *et al.*, *Sixth Catalog of Orbits of Visual Binary Stars*, on the WDS website. The fifth column references the published orbit that generated the ephemeris in question. Notes on residuals of special interest follow the table.

Table 4. Residuals from WDS and 2023 Ephemerides.

WDS ID	Name	Δ from WDS (θ, ρ)	Δ from 2023 Ephemeris	Orbital Ref.
02442+4914	STF296AB	-0.8°, 0.04″	0.2°, 0.73″	KSC2017
05003+3924	STT92AB	-0.1°, 0.12″	1.1°, -0.04″	Cve2006e
05013+5015	STF619	0.9°, 0.01″	0.3°, 0.13″	Kis2009
05172+3246	COU1088	-9.5°, -0.20″	N/A	N/A
06012+3516	HU826AB	8.8°, 0.32″	N/A	N/A
06012+3516	HO511AC	0.2°, 0.02″	N/A	N/A
09521+5404	STT208	-1.1°, -0.04″	-2.0°, -0.01″	Msn2021c
12115+5325	STF1608AB	0.0°, -0.03″	0.0°, -0.02″	Izm2019

12272+2701	STF1643AB	-1.1°, 0.04″	-0.1°, 0.05″	Ole2003b
12412-0127	BU607	-7.0°, -0.03″	N/A	N/A
12533+2115	STF1687AB	1.8°, -0.04″	1.7°, -0.05″	Izm2019
12533+2115	STF1687AC	-0.4°, 0.13″	N/A	N/A
13026+2318	COU95	-7.2°, 0.00″	N/A	N/A
13076-1415	RST3820	-3.2°, 0.00″	N/A	N/A
13120+3205	STT261	1.4°, 0.13″	0.6°, 0.01″	Izm2019
13152-1004	A2781	8.8°, -0.19″	N/A	N/A
13166+5034	STT263	-0.9°, -0.03″	-1.2°, 0.01″	Izm2019
13169+1701	BU800AB	0.3°, 0.08″	0.0°, 0.00″	Izm2019
13181-1820	RST2839AB	-17.1°, 0.10″	N/A	N/A
13199-2748	B247	-7.8°, 1.72″	N/A	N/A
13284+1543	STT266	3.5°, 0.05″	0.2°, 0.00″	Izm2019
13298-2634	B250	-3.6°, -0.01″	N/A	N/A
13375+3618	STF1768AB	-0.6°, 0.05″	0.4°, -0.04″	Izm2019
13400-1914	RST2858	-11.1°, -0.11″	N/A	N/A
13403-1913	RST2859	-0.1°, 0.01″	N/A	N/A
13491+2659	STF1785	1.5°, -0.10″	0.5°, -0.02″	Izm2019
14095-2205	RST2891	1.4°, -0.11″	N/A	N/A
14165+2007	STF1825	-2.1°, 0.13″	-0.6°, -0.03″	Izm2019
14247-1140	STF1837	-1.9°, -0.17″	-1.2°, -0.09″	Izm2019
14271-1505	RST3879	1.2°, 0.06″	N/A	N/A
14314+8257	MLR337	-0.1°, -0.03″	N/A	N/A
14381-0841	BU804	-0.6°, -0.06″	N/A	N/A
14447-0712	RST3893	-4.2°, -0.10″	N/A	N/A
14493-1409	BU106AB	1.1°, -0.05″	1.0°, -0.07″	Zir2015a
14579-2834	B283	-12.5°, 0.05″	N/A	N/A
15023-0858	RST3903	2.7°, -0.13″	N/A	N/A
15055+5707	A1113	0.3°, -0.06″	N/A	N/A
15055-0701	BU119AB	-0.1°, 0.01″	0.7°, -0.01″	Kiy2017
15199+6701	HU1161AB	2.2°, -0.27″	N/A	N/A
15304-2717	B292AB	2.6°, 0.05″	N/A	N/A
15304-2717	B292AC	-0.6°, 0.22″	N/A	N/A
15484-2210	B2370	-3.2°, 0.05″	N/A	N/A
16006-2027	HLD126	5.3°, -0.22″	N/A	N/A
16009+1918	A2081AB	3.5°, 0.02″	N/A	N/A
16011+6531	HU1170	0.7°, -0.27″	N/A	N/A
16044-1122	STF1998AB	4.6°, -0.12″	0.7°, -0.09″	Doc2009g
16044-1122	STF1998AC	-3.1°, 0.87″	-0.9°, 0.50″	Zir2008
16044-1122	STF1998BC	7.5°, -1.66″	N/A	N/A
16096-2037	HU660	-7.9°, 1.37″	N/A	N/A
16359-2510	RST3033	-6.1°, 0.15″	N/A	N/A

Notes:

05172+3246 COU1088: 3 WDS measures. The first two (from Couteau in 1974 & and Heintz in 1988) agree with one another in PA to within 0.6°, while the third (from TYCHO in 1991) differs from these by *ca.* +5.8°. The author's measures are closer to Couteau's in PA and Sep.

06012+3516 HU826AB: 6 WDS measures, from 1904 to 1981 which seem to show an increase in PA (300° to 308°) over 77 years (*i.e.* 0.1°/year). The author's measure would show a further increase to 312° in 42 years (also 0.1°/year). TYCHO measurements (1992) would decrease PA by 4.5° with respect to Heintz's (1981) at a rate of 0.4°/year. The author's Sep. increase is perhaps not real since there was no clear change in separation from 1904 to 1981. The companion double (HO511AC) shows good agreement with last published WDS measures made in 2015-16.

12412-0127 BU607: 18 WDS measures from 1867 to 1982. PA and Sep. show gradual decrease from 320° to 308°, and from 1.4 to 0.9 arcsec over the interval. The author's measures show no further clear decrease in Sep., but a continued decrease in PA. Long term PA decrease over 115 years was by about 0.1°/year; decrease since 1982 would be by 0.17°/year.

13026+2318 COU95: 12 WDS measures from 1966 to 2013, suggesting rapid decrease in PA (from 298° to 286° or 283°), and some increase in Sep. which may now have ceased (from 0.5 to 0.7 arcsec). Author's measures suggest continued rapid decrease in PA (to 279°), and no change in Sep.

13076-1415 RST3820: 2 WDS measures from 1937 and 1940. Author's measurement found no change in Sep., and modest 3° decrease in PA. "Relfix" over 85 years.

13152-1004 A2781: 9 WDS measures from 1914 to 1989, showing an increase of 17° in PA (0.23°/yr); and 0.2 to perhaps 0.4 arcsec in Sep. Author's measures show further increase of 9° in PA at roughly the same rate (0.26°/yr). Sep. is more in line with early measures than that of 1989. Possibly no real change in Sep. since 1914.

13181-1820 RST2839AB: 4 WDS measures from 1935 to 1960, with PA ranging from 32° to 48°, and Sep. from 0.3 to 0.5 arcsec, without clear temporal direction (*i.e.* there is scatter in the data). Author's present measurement, after an interval of 63 additional years, may show a real decrease in PA and increase in Sep. Further long term, high precision measurements could clarify the matter.

13199-2748 B247: 3 WDS measures from 1926 to 1960, showing PA decrease from 328° to 317°, and increase in Sep. from 1.8 to 2.5 arcsec. Author's recent measures show further PA decrease to 309° and Sep. increase to 4.3 arcsec, suggesting an optical pair with (perhaps) a linear solution.

13298-2634 B250: 8 WDS measures from 1926 to 1990. These show PAs from 41° to 49°, and Seps of 0.43 to 0.55 arcsec, without clear temporal direction. Author's measurements on two nights fall within this range at 42° and 0.54 arcsec. No clear movement after nearly 100 years.

13400-1914 RST2858: 2 WDS measures from 1935 and 1940, with PAs of 235° and 236°, and Sep. of 0.7 arcsec. Author's measures after 83 years show PA decrease of 11° and Sep. decrease of 0.1 arcsec. The nearby star RST2859, last measured in 2016, shows close agreement with the author's measures.

14095-2205 RST2891: 4 WDS measures from 1935 to 2016, perhaps showing an increase in PA from 136° to 141°, and Sep. from 0.6 to 0.9 arcsec. Author's measurement might show a slight further increase in PA to 142°.

14271-1505 RST3879: 2 WDS measures from 1937 and 1943, showing PA of 110° and Sep. of 0.7 arcsec. Author's measures show PA of 111° and Sep. of 0.8 arcsec, suggesting no clear movement after about 85 years.

14447-0712 RST3893: 4 WDS measures from 1938 to 1991. The first two are by Rossiter, the third by W. Heintz, and the last by HIPPARCOS, with PA decrease from 190° to 179°, and Sep. increase from 0.41 to 0.64 arcsec. The PA change would be at about 0.21°/yr. The author found a further decrease of 4° over 32 years giving a rate of 0.13°/yr, and a possible decrease in Sep. of 0.1 arcsec.

14579-2834 B283: 4 WDS measures from 1926 to 1962, showing a decrease in PA from 251° to 247° (0.09°/yr), and no clear change in Sep. Author's measures after an interval of 61 years show further decrease in PA to 235° (0.2°/yr) and no clear change in Sep.

15023-0858 RST3903: 3 WDS measures from 1938 to 2016, giving possible decreasing PA from 128° to 123°, and Seps steady at 1.2 arcsec. Author's measure would imply slight increase in PA and decrease in Sep. Perhaps, then, no real change since 1938. "Relfix."

15199+6701 HU1161AB: 7 WDS measures from 1905 to 1991, with a possible slight increase in PA from 222° to 225°, and Sep. from 1.5 to 1.7 arcsec. Author's measurements after 32 additional years suggest a further increase in PA to 227°, and possible decrease in Sep. to 1.4 arcsec.

15304-2717 B292AB: 3 WDS measures from 1926 to 1965, with PAs from 109° to 104°, and Sep. steady at 1.8 arcsec. Author's recent measurement closely accords, suggesting no clear movement in about 100 years.

15484-2210 B2370: 3 WDS measures from 1929 to 1959, possibly showing a slight decrease in PA by 2° (0.07°/yr), and no clear change in Sep. Author's measure after an interval of 64 years may show a further decrease in PA by 3° (0.05°/yr), but no clear change in Sep.

16006-2027 HLD126: 11 WDS measures from 1882 to 1991, showing no clear change in PA or Sep. Author's measures fall within the range of prior observations, also showing no clear movement of the pair after 140 years. "Relfix."

16009+1918 A2081AB: 8 WDS measures from 1909 to 1987, showing a gradual increase in PA from about 309° to 321° (0.15°/yr), and no clear change in Sep. over an interval of 78 years. Author's measures show a further increase in PA to 325° (0.11°/yr since 1987), but no clear change in Sep.

16096-2037 HU660: 10 WDS measures from 1902 to 1965, showing decrease in PA from 88° to 67°, and increase in Sep. from 1.8 to 2.6 arcsec. Author's measures show further decrease in PA to 59°, and increase in Sep. to 3.9 arcsec, suggesting an optical pair with (perhaps) a linear solution.

16359-2510 RST3033: 2 WDS measures from 1935 and 1940, with possible decrease of PA (from 150° to 146°), and increase of Sep. (from 0.5 to 0.6 arcsec). Author's measures would continue the trend (to 140° and 0.7 arcsec).

5. Non-detections

Table 5 lists fifteen systems in which the secondary was not detected by the author, although probably being within range of his 310-mm telescope.

Table 5. Non-Detection of Reported Secondaries

WDS ID	Name	JE	#Ims	#Nts
13137+2949	HO55AB	2023.42	5	1
13513-3315	RST2875	2023.45	3	1
14420-3249	SEE210AB	2023.45	6	1

14471-2729	B280	2023.47	5	1
14489-1247	RST3895	2023.42	5	1
14491-2228	B1765	2023.42	4	1
14506-2221	B1766	2023.48	5	1
15055-0501	HDS2125AB	2023.51	6	1
15139-2612	B288	2023.44	6	1
15195-2609	B289	2023.45	3	1
15343-1613	RST3923	2023.45	2	1
15475+7357	MLR194	2023.44	6	2
16152-0048	DOO62	2023.48	3	1
16164-2417	RST3010	2023.49	3	1
16500-2327	RST3045	2023.48	5	1

5. Acknowledgments

This research has made use of the Washington Double Star Catalog maintained at the U.S. Naval Observatory. The author wishes to thank the USNO, and Drs Brian Mason and Rachel Matson for their prompt and kind assistance. Also, F. Losse for the use of *REDUC*; T. Edelmann for *FireCapture*; and G. Sordiglioni for *Stelle Doppie*. The author also acknowledges and thanks *Stellarium*, and the SIMBAD database.

6. Images of Systems Measured

Below are images of double and triple systems taken through the author's 254-mm (first five images) and 310-mm (all remaining images) telescopes, demonstrating resolution of the stars.

(North toward bottom/east toward right)

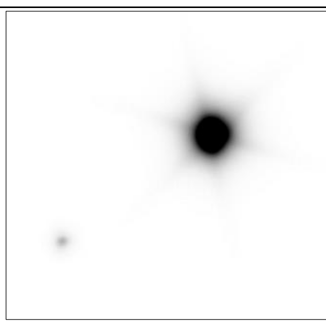

STF296AB

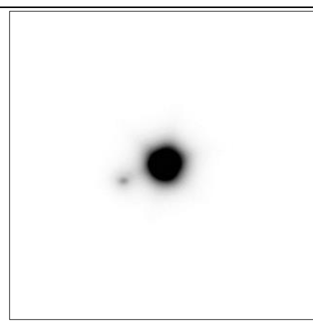

STT92AB

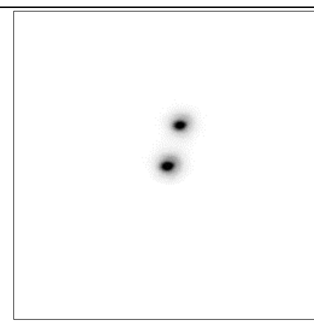

STF619

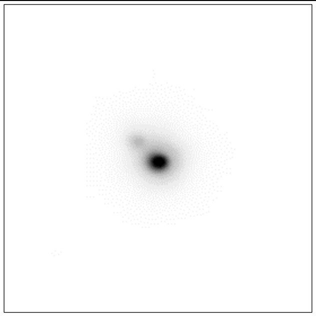 COU1088	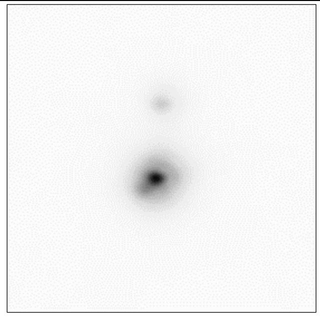 HU826AB + HO511AC	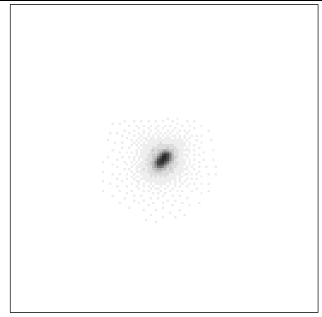 STT208
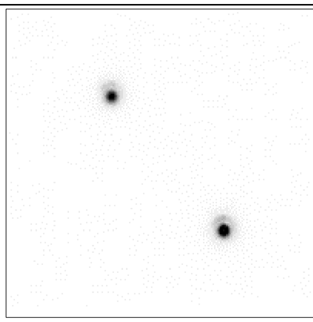 STF1608AB	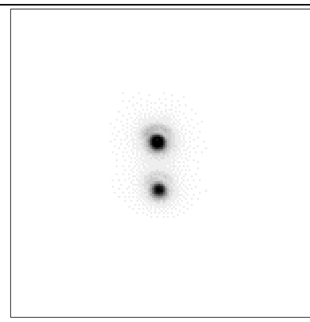 STF1643AB	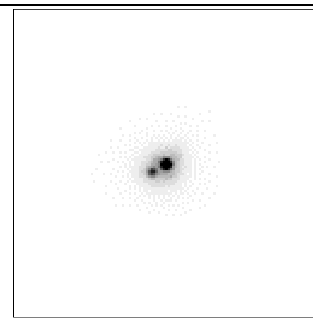 BU607
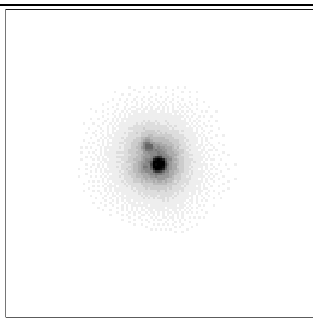 STF1687AB	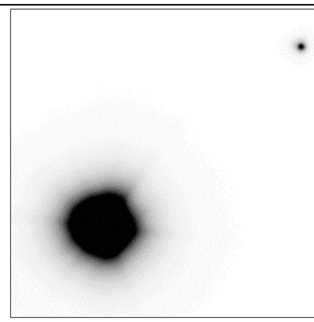 STF1687AC	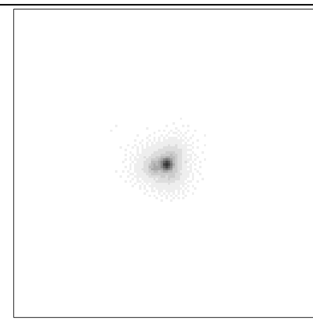 COU95
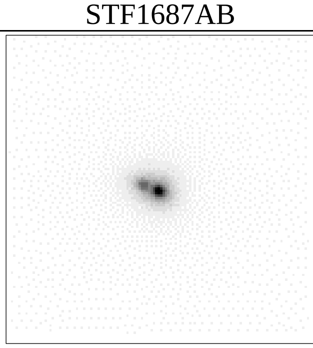 RST3820	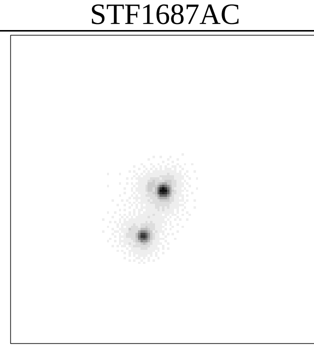 STT261	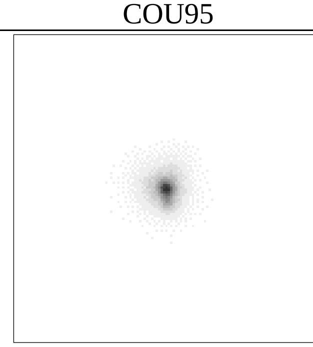 A2781

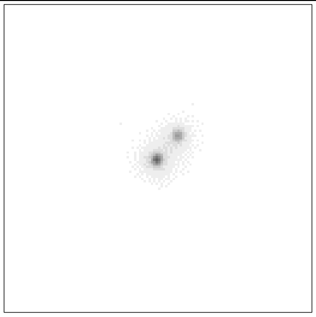 STT263	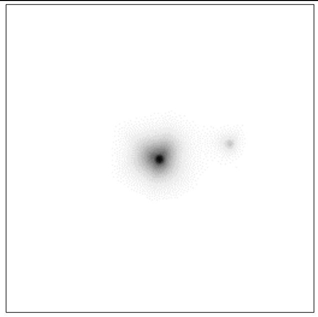 BU800AB	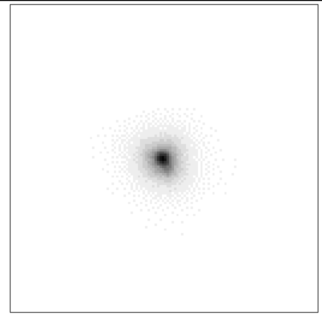 RST2839AB
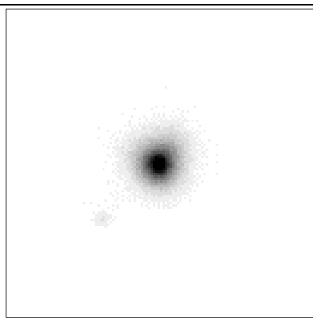 B247	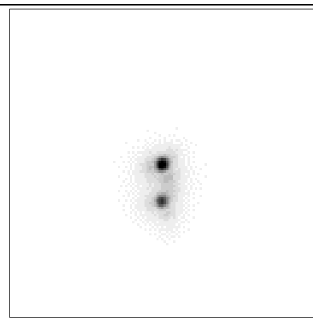 STT266	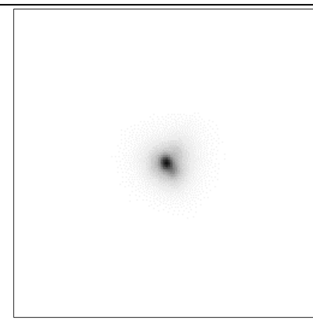 B250
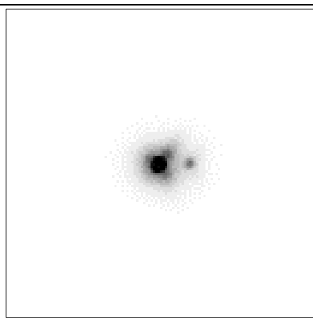 STF1768AB	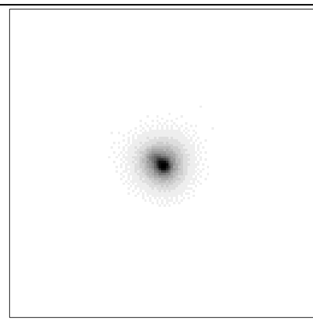 RST2858	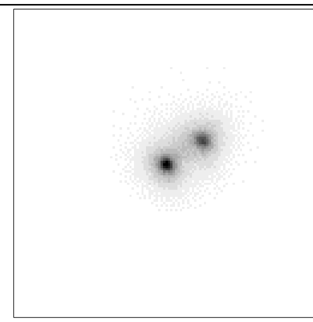 RST2859
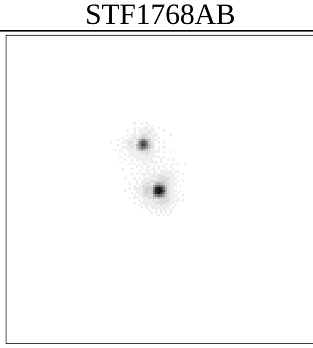 STF1785	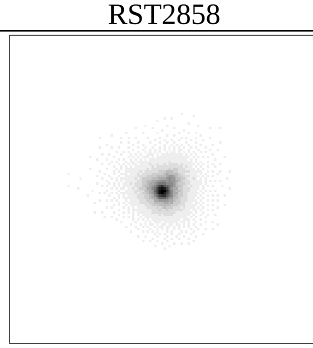 RST2891	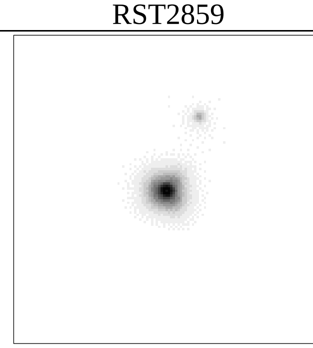 STF1825

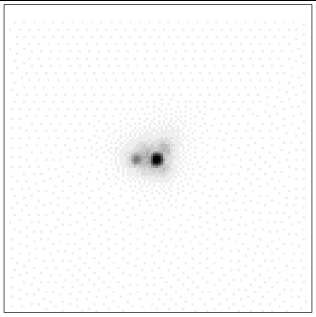
STF1837

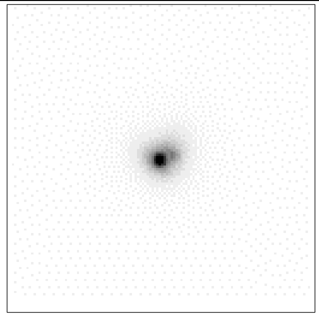
RST3879

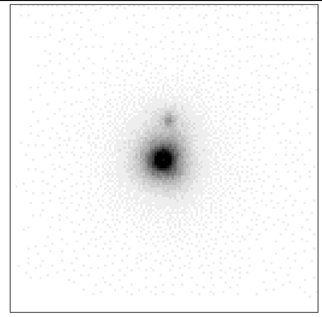
MLR337

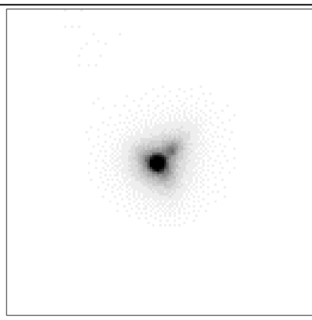
BU804

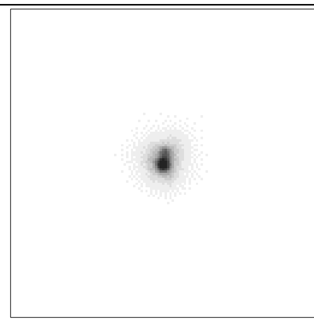
RST3893

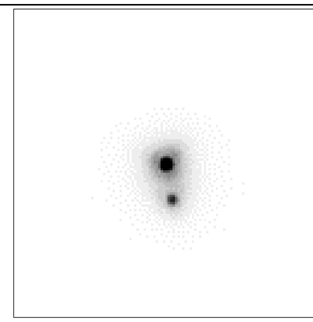
BU106AB

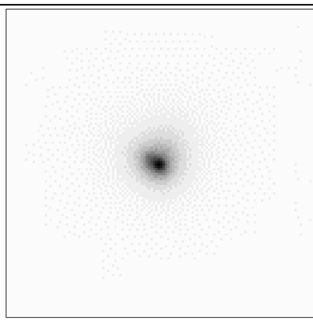
B283

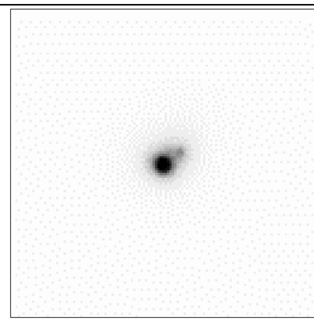
RST3903

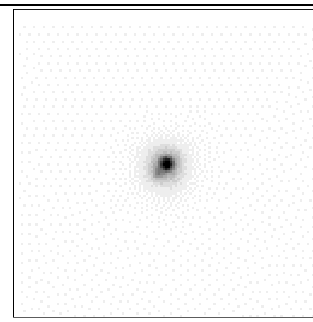
A1113

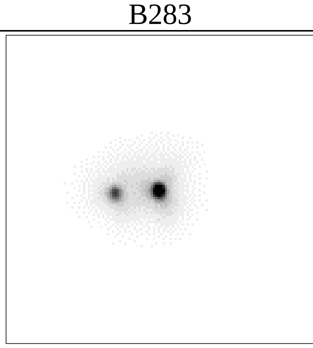
BU119AB

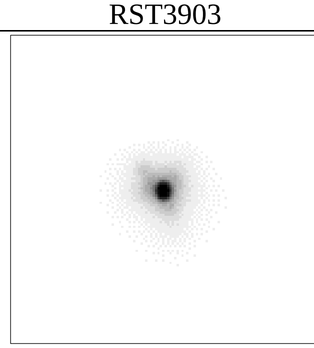
HU1161AB

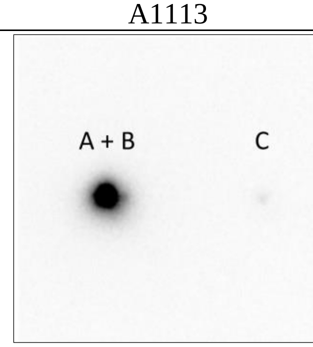

B292AB + C

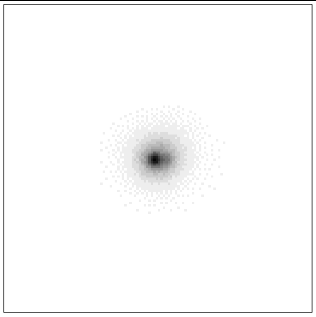
B2370

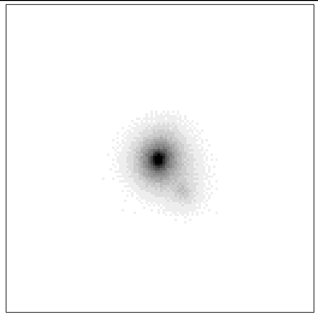
HLD126

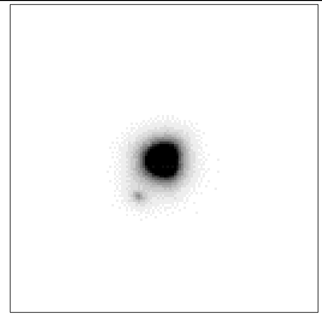
A2081AB

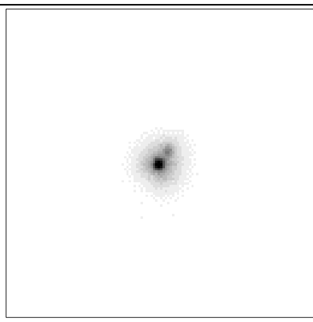
HU1170

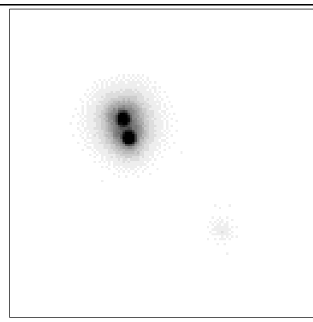
STF1998AB + C

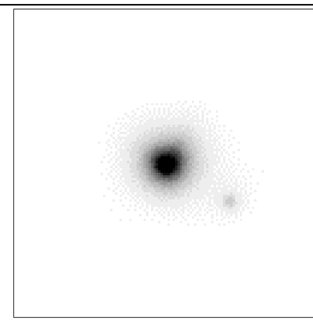
HU660

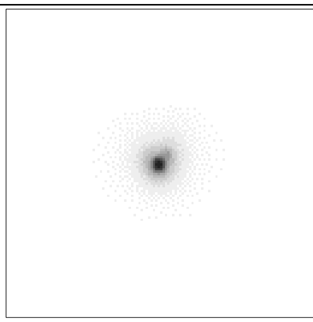
RST3033

Systems where reported secondary was not detected

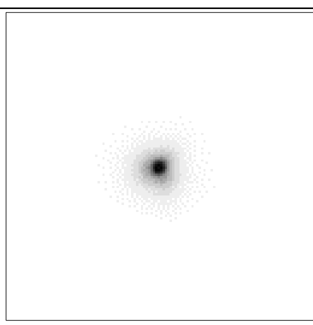
HO55AB

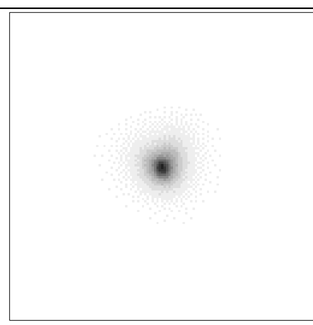
RST2875

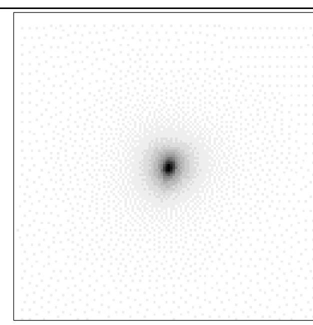
SEE210AB

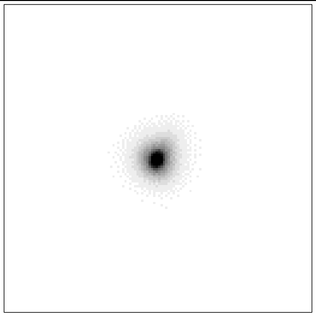
B280

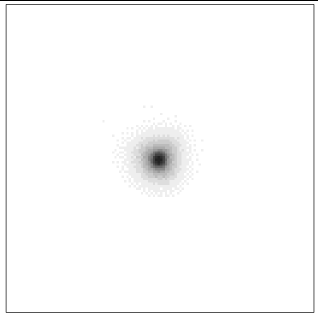
RST3895

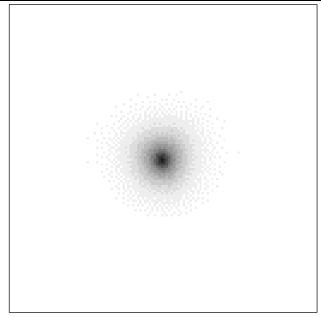
B1765

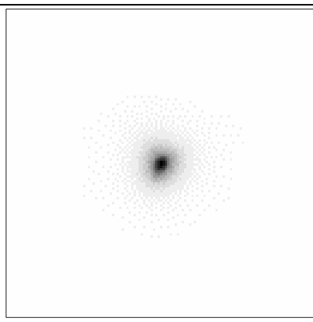
B1766

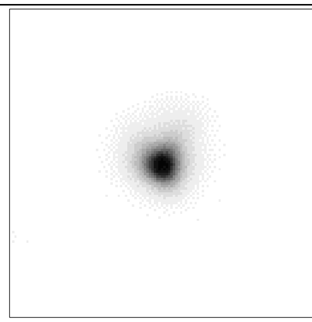
HDS2125AB

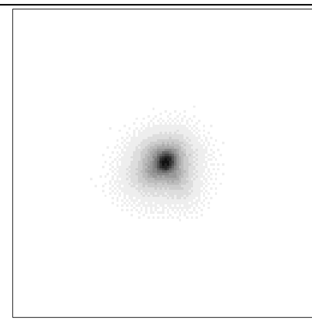
B288

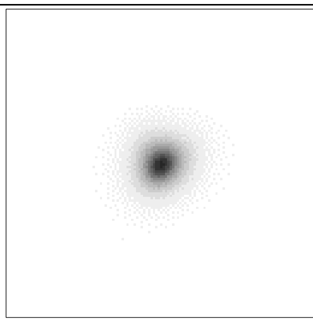
B289

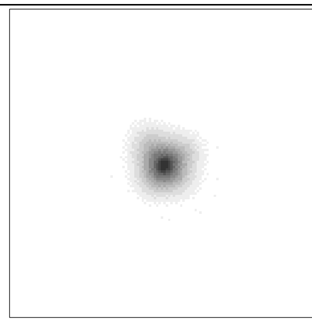
RST3923

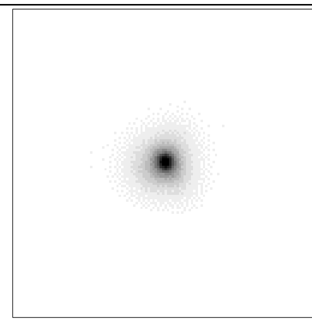
MLR194

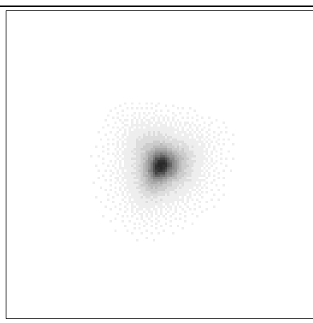
DOO62

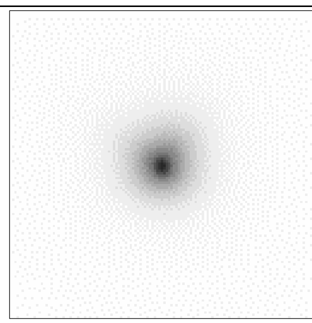
RST3010

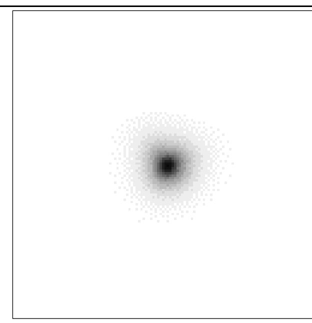
RST3045

References

Cotterell, J.D. (2015). "Calibrating the Plate Scale of a 20 cm Telescope with a Multiple-Slit Diffraction Mask." *Journal of Double Star Observations*, 11(4), 387-389.

Losse, F., "REDUC Tutorial," (V5.34). Retrieved from http://www.astrosurf.com/hfosaf/reduc/tutorial.htm

Mason, B.D. *et al*., "Washington Double Star Catalog." Retrieved from http://www.astro.gsu.edu/wds/

Matson, R.A., *et al*., *"Sixth Catalog of Orbits of Visual Binary Stars."* Retrieved from http://www.astro.gsu.edu/wds/orb6.html

Maurer, A. (2012). "The Diffraction Grating Micrometer." In R.W. Argyle (ed.), *Observing and Measuring Visual Double Stars*, (Springer), 183-193.

……………………………………..

About the author: Roger Ceragioli works as an optical engineer at the Richard F. Caris Mirror Lab, University of Arizona, Tucson, USA. His expertise is in optical fabrication and design, and he is in charge of diamond generating operations on the Giant Magellan Telescope's primary mirrors. He holds a Ph.D. from Harvard University.